ISSN: 0256-307X

中国物理快报
Chinese Physics Letters

Volume 27 Number 9 September 2010

A Series Journal of the Chinese Physical Society
Distributed by IOP Publishing

Online: http://www.iop.org/journals/cpl
http://cpl.iphy.ac.cn

CHINESE PHYSICAL SOCIETY

CHIN. PHYS. LETT. Vol. 27, No. 9 (2010) 094302

Pharmacokinetic Monitoring of Indocyanine Green for Tumor Detection Using Photoacoustic Imaging *

YANG Si-Hua(杨思华), YIN Guang-Zhi(阴广志), XING Da(邢达)**

MOE Key Laboratory of Laser Life Science and Institute of Laser Life Science, College of Biophotonics, South China Normal University, Guangzhou 510631

(Received 29 April 2010)

We report tumor detection using a photoacoustic technique for the imaging of angiogenesis and monitoring of agent pharmacokinetics on an animal model. We take 532-nm laser pulses to excite photoacoustic signals of blood vessels with acquisition by a broadband hydrophone, and the morphological characteristics of tumor angiogenesis are successfully image depicted. Furthermore, tumor pharmacokinetics is preformed and analyzed with fast multielement photoacoustic imaging of the intravenous-injected indocyanine green (ICG). Photoacoustic signals of ICG are excited with 805 nm laser pulses and recorded by transducer array as a function of time. The difference between the photoacoustic signal from the tumor side and that from the normal side is observed, and the ICG clearance velocity in the tumor area is found to lag behind that in the normal area. Experimental results demonstrate that photoacoustic imaging of morphological parameter and pharmacokinetics with specific agent may provide high sensitive approach for tumor detection and localization.

PACS: 43. 35. Ud, 42. 62. Be, 42. 30. Wb DOI: 10.1088/0256-307X/27/9/094302

Diagnosis of tumor is an important process of tumor therapy. In contrast to the normal region, tumor vasculature has an abnormal structure and function, such as the disorder of vascular and pharmacokinetic abnormal in the tumor. Different parameters in tumor growth are important for clinical diagnosis of tumor. There are many imaging modalities employed nowadays for tumor assess, including x-ray/CT, magnetic resonance imaging (MRI), positron emission tomography (PET) and near-infrared optical imaging. In comparison to the above imaging techniques, photoacoustic imaging (PAI) offers new approach for clinical diagnosis, and is noninvasive, relatively fast, economical and overcomes the high optical scattering of biological tissues. Photoacoustic imaging is a potentially powerful technique with excellent spatial resolution and satisfactory imaging depth, which combines high optical contrast and high ultrasound resolution into a single modality.[1,2] Absorption coefficients in tissues facilitate the discrimination of the malignant tissue from the normal tissue. PAI technique has been used for imaging tumor, brain and other diseases of blood vessels.[3–7] Our early work has achieved to high-resolution imaging of the developing vasculature during early tumor growth.[8,9]

Indocyanine green (ICG), a compound with FDA (food and drug administration), is of approval for systemic administration. ICG has been widely used in studies of cardiac defects, liver functions and ophthalmic diseases. When dissolved in blood, ICG binds to proteins such as albumin and lipoproteins, and the absorption maximum will from 780 nm shifts up to 805 nm. Some research has suggested that the angiogenesis process plays an important role in tumor growth, which implies that any further increase in tumor mass must be preceded by an increase of new capillary blood vessels which converge upon the tumor.[10–12] Since the ICG molecules are in the blood, the greater number of capillary blood vessels around tumors provides more ICG molecules around tumors and tends to collect in regions of dense vascularity through the enhanced permeation and retention (EPR) effect. In this case more PA signal is expected from the tumor tissue than from the healthy tissue.

The schematic of the experimental setup is shown in Fig. 1. Laser pluses with 532 nm and 805 nm are provided by a frequency doubled Nd:YAG laser and an optical parametric oscillator (VIBRANT B 532 I, OPOTEK, USA), which are used for exciting PA signals. A concave lens and a piece of ground glass are used to expend and homogenize the laser beam, so that the incident energy density is controlled below 20 mJ/cm^2. The incident laser beam on to the sample has a diameter of about 15 mm. Before experiment, general anesthesia was administered to the mouse by an intraperitoneal injection of pentobarbital, and the mouse is allowed to protrude into the water tank through a hole at the bottom of the tank and is insulated from the water by a piece of clear polyethylene membrane covering the hole. A sufficient

*Supported by the National Basic Research Program of China (2010CB732602), the Program for Changjiang Scholars and Innovative Research Team in University (IRT0829), the National Natural Science Foundation of China under Grant Nos 30627003 and 30870676, and the Natural Science Foundation of Guangdong Province (7117865).

**Email: xingda@scnu.edu.cn

amount of ultrasound gel was applied on the imaging area as an acoustic coupling medium for photoacoustic signals.

In the experiment of PA morphological imaging of tumor, a broadband needle hydrophone (Precision Acoustics Ltd, Dorchester, UK; diameter: 1 mm; sensitivity: 850 mV/Pa; bandwidth: 200 kHz–15 MHz) was used to capture the PA signals. The hydrophone is driven by a computer controlled stepper motor to scan around the mouse with 200 steps (1.8° per step) for high-precision scanning imaging. The received PA signals were amplified and recorded by a digital oscilloscope (TDS3032, Tektronix, USA), and then transmitted to a personal computer for subsequent data processing. In the experiment of PA pharmacokinetic monitoring, a 64-channel linear transducer array with effective length of 49 mm was used to receive PA signal. Each element of the array has a width of 0.3 mm, a pitch of 4 mm, and a center frequency of 2.5 MHz with a 70% bandwidth. PA signal from the array is captured by the home-made 64-channel parallel data-acquisition (PDA) equipment, which is employed to acquire, pretreat and transmit the measured raw PA signals. The linear transducer array is driven by a computer controlled stepper motor to scan around the mouse with 4 steps (90° per step) for the fast PA imaging. The signal acquisition time for one PA image with four-position collection including of the scanning time is about 2 s. PA signals after recorded in the PC, software of Matlab with the limited-view filtered back-projected algorithm was used to reconstruct the PA images.

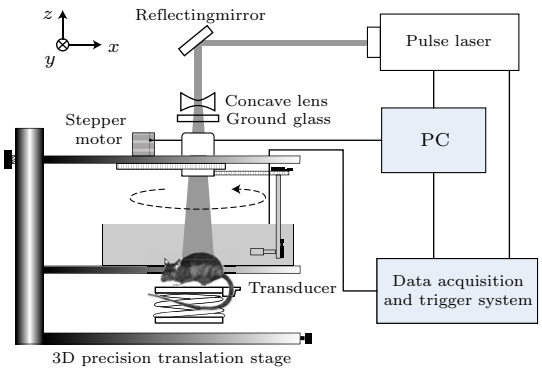

Fig. 1. Schematic diagram of the photoacoustic imaging system.

The S180 tumor model was generated by the subcutaneous injection of 4×10^7 cells in 50 μL PBS into the right hindlimb region of the female Balb/c mouse (about 26 g body weight). PA scanning was performed after tumor-cell inculcation for two weeks. The healthy region of the left hindlimb and tumor region of right hindlimb was PA scanned with the hydrophone respectively. Then ICG solution was intravenously injected into the tumor-bearing mouse tail for the PA pharmacokinetic imaging and monitoring.

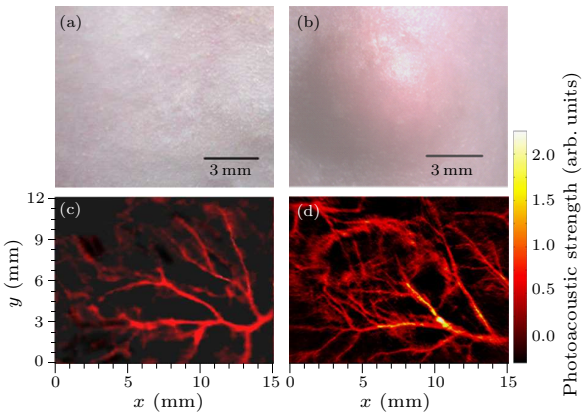

Fig. 2. *In vivo* photoacoustic images of vasculature in healthy region and tumor region on mouse hindlimb. (a) Photograph of the healthy left hindlimb. (b) Photograph of the tumor nodule on the right left hindlimb. (c) PA image of vasculature in healthy region. (d) PA image of angiogenesis in the tumor region.

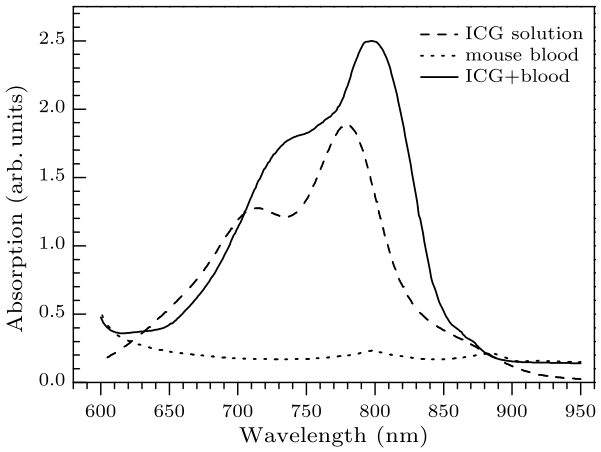

Fig. 3. Absorption spectra of ICG (200 μM), mouse blood and their mixture.

Figure 2 shows the *in vivo* microvascular network imaging by high-precision PA scanning imaging with 532-nm laser. Figures 2(a) and 2(b) are the photographs of the healthy and tumor region on the hindlimbs of a mouse two weeks after the tumor inoculation. The visual appearance of the tumor nodule is in oval shape, protruding over the skin surface by about 3 mm. Subcutaneous vasculature of the healthy region is clearly shown in Fig. 2(c), and obvious vessel branches are revealed by the PA image while they are invisible to the naked eyes in Fig. 2(a). Compared to Fig. 2(c), the morphological characteristics of tumor vasculature from Fig. 2(d) are different from those in healthy tissue. As can be seen, vascular networks in the tumor region are clearly resolved. Tumor blood vessels look highly disorganized, tortuous, dilated and excessive branching. The brighter colors indicate the

higher strength of PA signals, i.e. stronger absorbed optical energy density. Therefore, the morphological characteristics of the tumor side displayed in the PA image can conclude to high vessel density, high optical absorption, and ring-trend growth to the tumor mass, which are in agreement with those of tumor angiogenesis.[13,14] It can be concluded that the PAI technique is capable of imaging tumor angiogenesis *in vivo* and differentiate tumor tissue with high-resolution morphological characteristics.

To make PA detection of tumor more convincing, the pharmacokinetics of ICG was introduced to be explored with fast photoacoustic monitoring. Figure 3 shows the optical absorption spectral of mouse blood, ICG solution and the mixture of blood and ICG. The spectral distinctly validate that the absorption peak is shifted up to 805 nm when ICG binding to blood proteins, and great higher absorption of ICG than that of blood in the near-infrared region is clearly revealed. Therefore, 805 nm laser pluses were choose to stare the PA signal of ICG. We injected 100 μL ICG solution (200 μM) to the mouse body through the tail vein before the experiment. Continuous PA monitoring of tumor region and healthy region with the transducer array were performed, respectively.

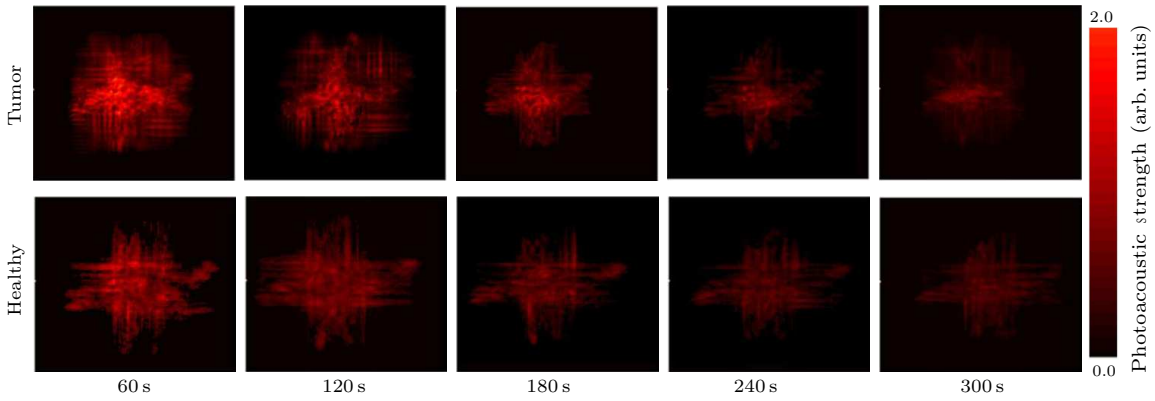

Fig. 4. *In vivo* PA imaging of ICG pharmacokinetics on the tumor and healthy region of the mouse hindlimbs. Reconstructed images are collected after injection of ICG with 60 s, 120 s, 180 s, 240 s, 300 s.

Photoacoustic monitoring of ICG clearance in tumor and normal region was achieved with reconstruction by 4 rotated scanning positions and shown in Fig. 4. The PA image slices with interval of 60 s indicate different uptake of ICG in the tumor and normal tissue. For the sake of giving intuitionistic contrast of dynamic of ICG, the strength of PA signals are displayed. Strength of photoacoustic signal, which reflected the optical absorption in vessel at 805 nm wavelength, can also reflect the concentration of ICG in tissue. Figure 5 shows the typical PA signal curve as a function of time, and the line of square and the line of rotundity represent the PA signal from the normal region and tumor region, respectively. It is noted that the PA signal reaches the maximum of about 20 s after injection of ICG, and that the PA signal from the tumor side is higher than that from the normal side, which suggests more ICG molecules are around the tumor than in the surrounding normal tissue. The PA signal decreases after reaching maximum since the ICG are cleared up by the liver cells through the blood circulation. Most important, different dynamical feature was observed for the physiological state. There are about 100 s intervals of the characteristic decay time between the normal and the tumor side. The tumor cases exhibited slower rate of ICG clearance compared to the healthy tissue. The results show that the PAI can continuously monitor the dynamics of ICG *in vivo*, and has potential to distinguish tumor and healthy tissue with pharmacokinetic characteristics.

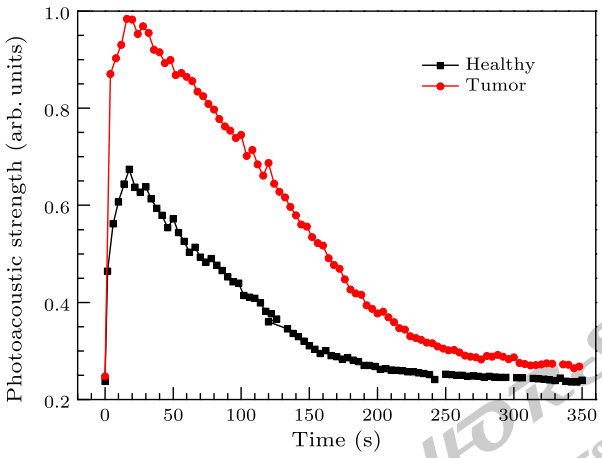

Fig. 5. PA signal curve as a function of time. The upper curve is the PA signal from tumor side and the lower curve is the PA signal from the healthy side.

In summary, morphological features and pharmacokinetics of ICG for inoculated tumor on the mouse model have been clearly revealed with single and multielement photoacoustic imaging systems, respectively. These results demonstrate that photoacoustic

imaging has the potential to become a useful tool in detecting tumor and monitoring the process of anti-angiogenic therapy.

References

[1] Razansky D, Distel M, Vinegoni C, Ma R, Perrimon N, Kvster R W and Ntziachristos V 2009 *Nature Photon.* **3** 412

[2] Zhang H F, Stoica M G and Wang L H 2006 *Nature Biotechnol.* **24** 848

[3] Yang D W, Xing D, Yang S H and Xiang L Z 2007 *Opt. Express* **15** 15566

[4] Chen X, Tang Z L, He Y H, Liu H F, Wei Y D and Wu Y B 2009 *J. Biomed. Opt.* **14** 059801

[5] Su Y X, Zhang F, Xu K X, Yao J Q and Wang R K 2005 *J. Phys. D: Appl. Phys.* **38** 2640

[6] Yang S H, Xing D, Zhou Q, Xiang L Z and Lao Y Q 2007 *Med. Phys.* **34** 3294

[7] Yang S H, Xing D, Lao Y Q, Yang D W, Zeng L M, Xiang L Z and Chen W 2007 *Appl. Phys. Lett.* **90** 243902

[8] Lao Y Q, Xing D, Yang S H and Xiang L Z 2008 *Phys. Med. Biol.* **53** 4203

[9] Xiang L Z, Xing D, Gu H M, Zhou F F, Ying D W, Zeng L M and Yang S H 2007 *Chin. Phys. Lett.* **24** 751

[10] Hawrys D and Sevick-Muraca E 2000 *Neoplasia* **2** 388

[11] Motomura K, Inaji H, Komoike Y, Kasugai T, Nogushi S and Koyama H 1999 *Jpn. J. Clin. Oncol.* **29** 604

[12] Intes X, Ripoll J, Chen Y, Nioka S, Yodh A G and Chance B 2003 *Med. Phys.* **30** 235

[13] Delorme S and Knopp M V 1998 *Eur. Radiol.* **8** 517

[14] Less J R, Skalak T C, Sevick E M and Jain R K 1991 *Cancer Res.* **51** 265

Chinese Physics Letters

Volume 27 Number 9 2010

GENERAL

NUCLEAR PHYSICS

(Continued on inside back cover)

ATOMIC AND MOLECULAR PHYSICS

FUNDAMENTAL AREAS OF PHENOMENOLOGY(INCLUDING APPLICATIONS)

PHYSICS OF GASES, PLASMAS, AND ELECTRIC DISCHARGES

CONDENSED MATTER: STRUCTURE, MECHANICAL AND THERMAL PROPERTIES

CONDENSED MATTER: ELECTRONIC STRUCTURE, ELECTRICAL, MAGNETIC, AND OPTICAL PROPERTIES

CROSS-DISCIPLINARY PHYSICS AND RELATED AREAS OF SCIENCE AND TECHNOLOGY

GEOPHYSICS, ASTRONOMY, AND ASTROPHYSICS